Internal Features of Fiber Fuse in a Yb-Doped Double-Clad Fiber at 3 kW *

Qi-Rong Xiao(肖起榕), Jia-Ding Tian(田佳丁), Yu-Sheng Huang(黄昱升), Xue-Jiao Wang(王雪娇), Ze-Hui Wang(王泽晖), Dan Li(李丹)**, Ping Yan(闫平), Ma-Li Gong(巩马理)

Center for Photonics and Electronics, Department of Precision Instrument, Tsinghua University, Beijing 100084

(Received 18 December 2017)

We study internal features of fiber fuse in a Yb-doped double-clad fiber. The samples of fiber fuse are acquired at the power level of 3 kW in an all-fiber forward-pumped master oscillator power amplifier configuration fiber laser that is built specially for fiber fuse analyses. At this high power level, drastic refractive-index redistribution arises in an expended high refractive index area around the bullet-shaped voids of fiber fuse. Electron spin resonance analyses on post-fiber-fuse samples of the Yb-doped double-clad fiber indicate rising Frenkel defect concentration, meanwhile showing a new resonance center that is different from the ones of the Ge-doped fibers studied previously. This new resonance center probably suggests the generation of Al-oxygen hole center, a kind of defect formed during the catastrophic fuse process.

PACS: 42.81.−i, 42.55.Wd, 71.55.−i, 61.72.Hh DOI: 10.1088/0256-307X/35/5/054201

High power fiber lasers, due to their near-diffraction-limit beam quality, high optic-to-optic efficiency, and compactness, have yielded extensive applications in the military, industry, medicine, and so on. Nevertheless, the power scaling of high power fiber lasers while maintaining excellent beam quality has been obstructed by several inherent factors, such as fiber fuse, mode instability, and Raman scattering. Among them, fiber fuse, visually similar to a burning fuse, can cause catastrophic destruction to optical fiber by vaporizing fiber core and leaving a series of voids behind.[1] As a consequence, the fiber laser would receive irreversible damages and lost ability of proper function.

Fiber fuse was first observed in 1980.[2] Although it has been more than 30 y since then, no agreement has been reached in the generation mechanism of fiber fuse. One main reason is the lack of experimental data. Therefore, worldwide researchers have taken endless efforts to study this destructive phenomenon. Among them, a huge part of the research on fiber fuse focused on the external features of fiber fuse and its consequence, such as velocity, threshold power, and the distribution pattern of periodic voids in the fiber.[3−7] Moreover, there has also been considerable research trying to find insight into deeply. In 1987, Kashyap analyzed the remnant cavity in a Ge-doped fiber after fiber fuse and discovered the presence of molecular oxygen.[3] In 1988, Hand and Russell found out a strong trail of GeE' in Ge-doped fiber after fiber fuse, suggesting the important role point defect plays in fiber fuse.[4] In 2004, Shuto *et al.* revealed that the origin of fiber fuse in a Ge-doped fiber, which is the significant increase of the optical absorption, could be induced by several factors including thermal ionization and silica decomposition.[8]

Although various researches have made significant progress in the investigation of fiber fuse, most of the current studies are only concerned with the fiber fuse in inactive fiber, for example, Ge-doped fiber, polymer optical fiber, and photonic crystal fiber.[3−10] Moreover, these researches mostly cover the fiber fuse at the power level as low as several watts and power density of merely a few MW/cm^2, because they chiefly focus on the fiber fuse that took place in the optical communication system.

Recently, due to rising interest in high power fiber laser, researches on fiber fuse began to shift their attention to Yb-doped fiber (YDF).[11] Wang *et al.* in 2008 presented the observation result of fiber fuse in high numerical aperture (NA) double-clad YDF.[12] In 2013, Zhang *et al.* observed fiber fuse in a large mode area double-clad YDF at the output power of 400 W.[13] However, the power level of these researches is still confined to a few hundreds of watts, leaving a blank space in both external and internal features studies in kW level fiber fuse phenomenon because of extremely high demand on the experimental condition and high fiber damage cost.

Our group has been focusing on the high power fiber laser for a long time and also noticed that fiber fuse could be a serious threat to the stable running of high-power fiber laser systems.[14−16] Accordingly, we are able to carry out researches on high power fiber fuse, especially in YDF. In 2016, we reported the investigation of external features of fiber fuse in double-clad YDF at the kW power level.[17]

In this work, we present the study on fiber fuse in YDF at 3 kW high power level, for the first time to our knowledge. A 3 kW power level all-fiber forward-pumped master oscillator power amplifier (MOPA) configuration laser was built specially to acquire the

*Supported by the National Natural Science Foundation of China under Grant Nos 61675114 and 11604177, the Key Laboratory of Science and Technology on High Energy Laser and China Academy of Engineering Physics under Grant No 2014HEL02, and the Tsinghua University Initiative Scientific Research Program under Grant No 20151080709.

**Corresponding author. Email: dli@mail.tsinghua.edu.cn

© 2018 Chinese Physical Society and IOP Publishing Ltd

experimental sample for further fiber fuse analyses. The fiber fuse was triggered off in the YDF while the laser system was working. After the fiber fuse, refractive index (RI) profiles and electron spin resonance (ESR) spectra of the YDF samples were collected to reveal the internal features of the catastrophic fuse process. Firstly, the RI profiles of both before and after fiber fuse YDF were measured. The results displayed significant RI redistribution in the bullet-shaped voids caused by fiber fuse where the center was emptied and the RI rose drastically in an expanded 'core' due to the various factors. Furthermore, the comparative ESR analyses of YDF before and after fiber fuse suggested a significant rise in the Frenkel defect concentration after fiber fuse. From the results, we also discover an absorption center that has never been observed in Ge-doped fiber ESR analyses, which was speculated to be the sign of Al-oxygen hole center (AlOHC) originated from the co-dopant Al in the YDF. These analyses added to the experimental data of fiber fuse, especially in the case of YDF at high power situations. Hopefully, it will promote further exploration into the mechanism of fiber fuse.

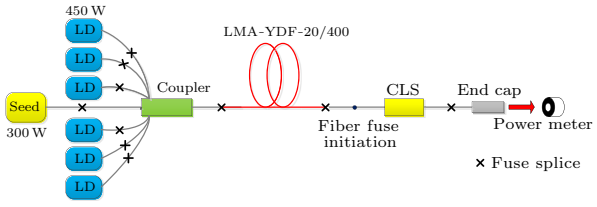

Fig. 1. Schematic diagram of experimental setup of post-fiber-fuse fiber sample preparation.

To acquire the YDF sample after high power fiber fuse, we built a 3 kW all-fiber continue-wave MOPA fiber laser, as illustrated in Fig. 1. A 1080 nm fiber oscillator is served as the seed laser. The seed laser was coupled into a one-stage amplifier through a $(6+1)\times 1$ pumping coupler. A 25-m-long Yb-doped double-clad large-mode-area fiber was employed as the gain medium of the amplifier, with a core and clad diameter of 20/400 μm and a core and clad NA of 0.06/0.46. Six 976 nm laser diodes each with a maximum power of 450 W provided pumping power for the amplifier, and an end cap with a diameter of 400 μm was used at the output end of the amplifier.

As the seed laser provided a power of 292 W, a maximum output power of 3130 W was achieved by the laser system when a total of 3895 W pumping power was launched, corresponding to an optical-to-optical efficiency of 80.4%, as depicted in Fig. 2. The power intensity inside the core of the YDF reached as high as 996.3 MW/cm^2. The average propagating velocity of the fiber fuse is 14.4 m/s.

The initiation point of fiber fuse is on a section of passive fiber where the polymer coating was removed by 1 cm, as depicted in Fig. 3(a). At the maximum output power 3 kW, a piece of metal as absorptive material is manually put on the exposed inner clad. The fiber fuse is initiated immediately. The light that propagates in the inner clad is guided into the material, and absorbed, that leads to temperature rise, which finally triggers the onset of fiber fuse. The initiated fiber fuse propagates toward the laser sources. As can be seen in Fig. 3(b), the propagating fiber fuse generates strong light, illuminating the whole background. When the fiber fuse is terminated by shutting down the laser, a 1 m post-fiber-fuse YDF sample is acquired near the output end. An intact YDF sample of the same length is also prepared as a control material.

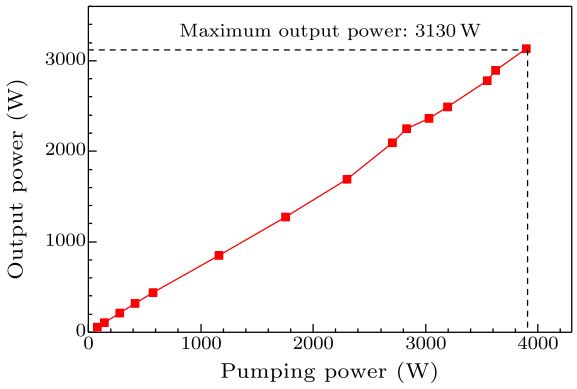

Fig. 2. Output power versus pumping power of the 3 kW fiber laser.

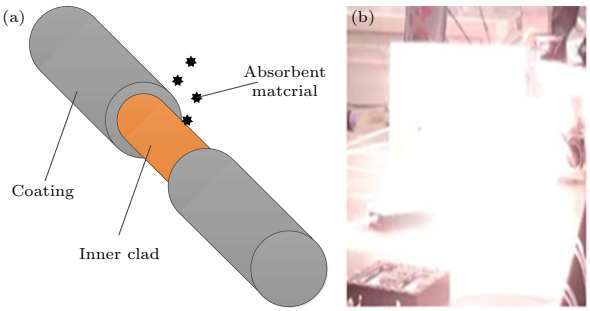

Fig. 3. Schematic diagram of fiber fuse initiation point (a), and the photo of the fiber fuse phenomenon (b). The white square in (b) is a metal plain illuminated by the propagating fiber fuse.

It can be observed with a microscope that the post-fiber-fuse sample is greatly damaged and left with a series of non-periodic bullet-shaped voids in the core area, as depicted in Fig. 4. As a consequence, fiber fuse causes permanent and irreversible change to the internal structure and transmission feature of the optical fiber.[18] To investigate what degree the fiber fuse alters the waveguide structure of YDF, we measured the relative RI profiles of both before and after fiber fuse YDF samples via an S14 RI profiler using a refracted near field technique, as shown in Fig. 5. The measurement of RI profiles in the post-fiber-fuse sample is taken near the narrow end and the broad end of the bullet-shaped void. As shown in the results, the previous even RI distribution in the fiber core is evidently altered. The index profile in the central area is reduced, which obviously results from the decom-

position of silica. In addition, near the relative low-RI area, the RI rapidly rises and is higher than the original RI of the inner cladding. Also, the size of the relative high-RI area (∼50 μm) is larger than that of the original fiber core (20 μm). There are several reasons for this rise, one of which is the new generated SiO gasified from the high temperature of fiber fuse and adhered to the adjacent shell of the bullet-shape void.[5] The redistribution of doped rare-earth material and the compression and densification of silica may also be responsible for this RI rise.[19] The possibility of contaminated samples for this RI rise could be excluded by carefully cleaning the samples.

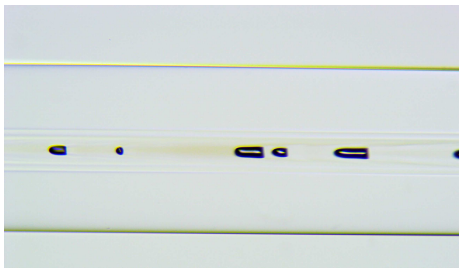

Fig. 4. Microscopic images of the YDF sample after fiber fuse. The image was taken with the fiber sample immersed in RI match oil.

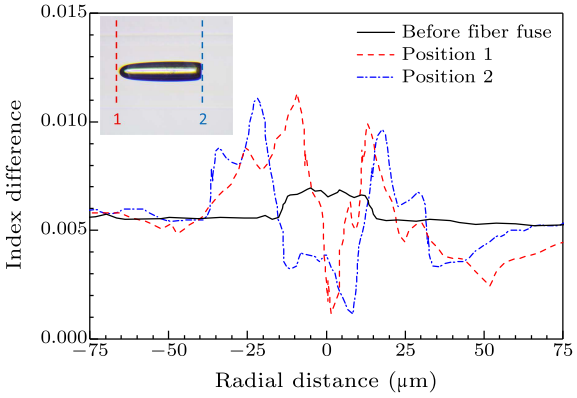

Fig. 5. Relative RI profile of YDF before fiber fuse sample and after fiber fuse samples at two positions of the bullet-shaped void. The positions where the measurement was performed were marked in the inset picture.

To further explore the inherent changes that take place during the fiber fuse phenomenon, a series of ESR spectra were conducted on both samples with a JES-FA200 ESR spectrometer. After the removal of the outer coating, the samples were cut into pieces less than 4 cm to fit the effective measurement zone. The microwave used in the measurement had a frequency of 9053.706 MHz. The measurements were performed under the condition of a 100 kHz field modulation at room temperature.

To avoid signal saturation, we started with the comparison of a series of ESR spectra of samples measured under different microwave powers, as shown in Fig. 6. First, the ESR intensity becomes stronger when the microwave power gradually rises from 5 μW to 20 μW where the maximum peaks occur. Then the ESR intensity turns weaker as the microwave power increases from 20 μW. Thus the appropriate working microwave power of ESR spectra measurement is chosen to be 20 μW.

Then, the ESR spectrum of the YDF sample before fiber fuse is investigated, as shown in Fig. 6. We define the spectrum with the g values of the first peak, the second peak, the zero point and the valley, which are listed in Table 1. According to previous studies, the resonance centers in Fig. 6 also exist in the ESR spectrum of Ge-doped fiber, which is attributed to the Frenkel defect, also known as E'-center.[20,21] The E'-center is mainly induced to the optical fiber at high temperature during the drawing process, which can be described as follows:[7]

$$X-\mathrm{O}-\mathrm{Si}\rightarrow X^{\bullet}\mathrm{Si}^{+}+\left(\frac{1}{2}\right)\mathrm{O}_2\uparrow+e^{-}. \qquad (1)$$

As for the case of YDF, X in Eq. (1) can stand for Si or Yb. The E'-center is caused by the break of the O–X–O bond. The electrons, released during the thermal ionization process in Eq. (1), will lead to the increase of electrical conductivity and thus optical absorption. Therefore, the existence of E'-center is reckoned as a contributing factor for the fiber fuse effect.[8]

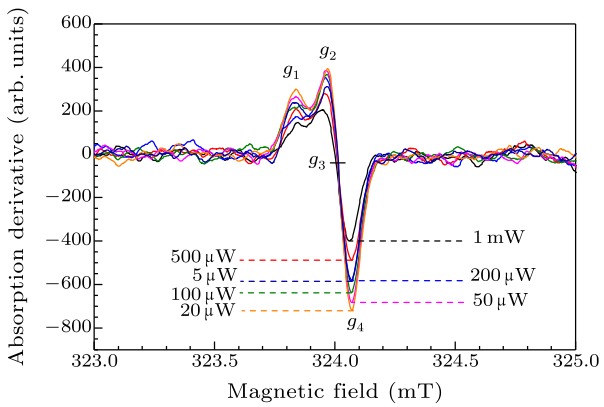

Fig. 6. ESR spectra of YDF under different microwave powers.

Table 1. The values of g of E'-centers. Here the values of g are calculated by the expression $g = h\nu/\mu_{\mathrm{e}}H_0$, where h is the Plank constant, ν is the microwave frequency used in the ESR analyses, μ_{e} is the Bohr magneton, and H_0 is the strength of the applied magnetic field.

g_1	g_2	g_3	g_4
2.0012	2.0004	2.0002	1.9998

As depicted in Fig. 7, the ESR spectrum of YDF after fiber fuse reveals evident changes compared with the spectrum before fiber fuse. On the one hand, the ESR intensity of E'-centers in the post-fiber-fuse sample is significantly stronger than the before-fiber-fuse sample, indicating the generation of a large amount of E'-center after fiber fuse. At the same time, we manage to capture the trail of the released oxygen in Eq. (1) in the bullet-shaped void of the post fiber fuse

YDF sample with the analyses of Raman spectrum. The analyses were performed on a LabRAM HR Evolution Raman spectrometer. The laser wavelength employed by the spectrometer was 632.8 nm and the spectral resolution was 0.65 cm^{-1}. The spatial resolutions were 1 μm and 2 μm in the transverse and longitudinal direction, respectively. The laser was focusing at the center of the void in the sample. As shown in Fig. 8, compared with the Raman spectrum of YDF before fiber fuse arises, a peak around the Raman shift of 1555 cm^{-1} emerges after the fiber fuse, which is suspected to be the sign of oxygen.[3]

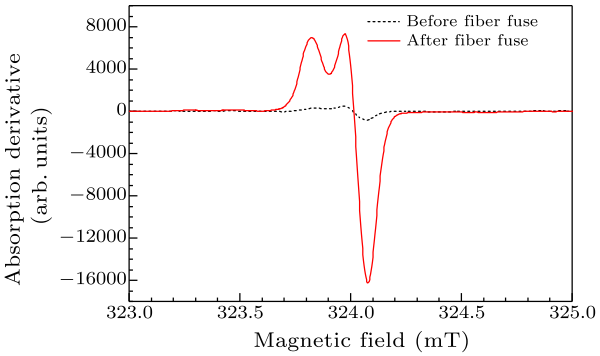

Fig. 7. E'-center signal in the ESR spectra of YDF samples before and after fiber fuse. The measurements were both conducted under the microwave power of 20 μW.

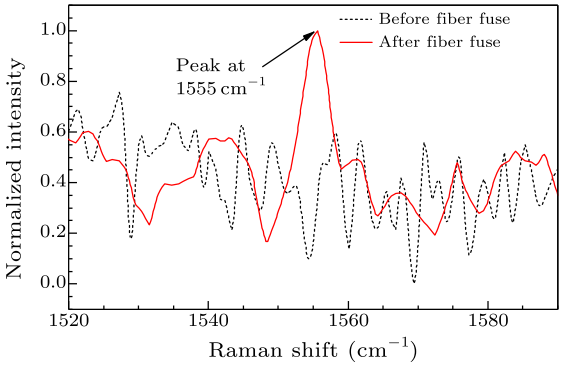

Fig. 8. Raman spectrum analysis at the bullet-shaped void in the post-fiber-fuse YDF (solid) and before-fiber-fuse YDF sample (dashed).

On the other hand, we observed a new resonance center appearing in the post-fiber-fuse sample, as depicted in Fig. 9, whose g values are listed in Table 2, which has never occurred in the ESR studies of Ge-doped fibers before or after fiber fuse.[20,21] Thus this spectrum may indicate chemical changes related to dopant Yb or materials that only exist in YDF.

Comparing the ESR spectrum with previous researches, we speculate that this new resonance center may be attributed to AlOHC which most likely comes from the Al co-dopant in the YDF.[22] On the one hand, the AlOHC can be induced by extreme stimulations like γ-radiation, thus there is the possibility that it is a product of extreme thermal and radiation environment during the fiber fuse process. On the other hand, if the AlOHC was generated before fiber fuse took place, stimulated by the rising temperature or laser power, it can act as a contributing role in triggering fiber fuse because AlOHC can lead to a rising optical absorption.[22,23] Similar to the mechanism of E'-center in fiber fuse proposed by Shuto *et al.*,[8] it can be another cause for fiber fuse specifically in YDF. Thus our future work will focus on figuring out whether the AlOHC is generated before or during fiber fuse.

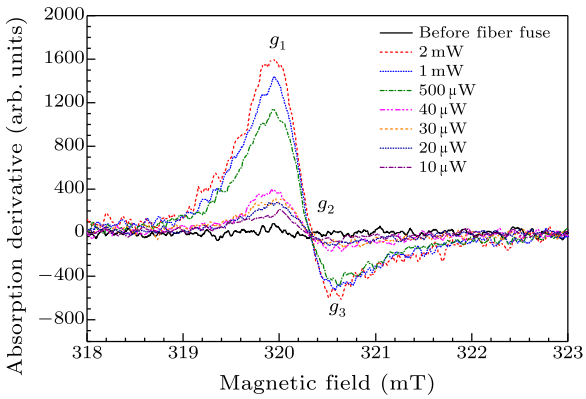

Fig. 9. New resonance centers in the ESR spectra of the post-fiber-fuse YDF sample under different microwave powers in comparison with the ESR spectra of YDF before fiber fuse.

Table 2. The values of g of the resonance centers in Fig. 9.

g_1	g_2	g_3
2.0257	2.0248	2.0230

In summary, we have investigated the changes of internal features of fiber fuse in YDF at the power level of 3 kW, including RI profile and ESR spectrum. The RI profile of the bullet-shaped voids in the post-fiber-fuse sample shows a rearranged RI profile that is hollow at the center and evidently high in an expanded high RI area, mostly due to the decomposition of SiO_2 (accordingly releasing SiO and oxygen), redistribution of dopants, and compression of silica. The comparison of ESR spectra analyses of YDF before and after fiber fuse reveals an increasing concentration level of the Frenkel defects after fiber fuse. The ESR spectrum of the post-fiber-fuse YDF sample also captures a new resonance center that has never been observed in Ge-doped fibers, which is most likely to belong to AlOHC. To the best of our knowledge, this is the first study of internal features of fiber fuse in YDF, and especially at the kW power level. These results will help to build the experimental data for further exploration on the generation mechanism of fiber fuse in YDF.

References

[1] Kashyap R 2013 *Opt. Express* **21** 6422
[2] Kashyap R and Blow K J 1988 *Electron. Lett.* **24** 47
[3] Kashyap R 1988 *Proc. Tenth Int. Conf. Lasers Appl. McLean VA* 859

[4] Hand D P and Russell P St J 1988 *Opt. Lett.* **13** 767
[5] Hand D P, Townsend J E and Russell P St J 1988 *Digest of Conference on Lasers and Electro-Optics* (Anaheim, US) p WJ1
[6] Atkins R M, Simpkins P G and Yablon A D 2003 *Opt. Lett.* **28** 974
[7] Jiang S L, Ma L, Fan X Y et al 2016 *Sci. Rep.* **6** 6
[8] Shuto Y, Yanagi S, Asakawa S et al 2004 *IEEE J. Quantum Electron.* **40** 1113
[9] Hanzawa N, Kurokawa K, Tsujikawa K et al 2010 *J. Lightwave Technol.* **28** 2115
[10] Mizuno Y, Hayashi N, Tanaka H et al 2014 *Appl. Phys. Lett.* **104** 043302
[11] Wang J, Gray S, Walton D et al 2008 *Asia Pac. Opt. Commun. Hangzhou Chin.* 71342E
[12] Liao L, Liu P, Xing Y B et al 2015 *Chin. Phys. Lett.* **32** 064201
[13] Zhang H, Zhou P, Wang X et al 2013 *Conf. on Lasers and Electro-Optics/Pacific Rim* (Kyoto, Japan, JETP) p WPD4
[14] Yan P, Yin S, He J et al 2011 *IEEE Photon. Technol. Lett.* **23** 697
[15] Xiao Q R, Yan P, Li D et al 2016 *Opt. Express* **24** 6758
[16] Wang X J, Xiao Q R, Yan P et al 2015 *Acta Phys. Sin.* B **24** 164204 (in Chinese)
[17] Sun J Y, Xiao Q R, Li D et al 2016 *Chin. Phys.* B **25** 014204
[18] Dianov E, Mashinsky V, Myzina V et al 1992 *Sov. Lightwave Commun.* **10** 118
[19] Bufetov I A, Frolov A A, Shubin A V et al 2008 *Quantum Electron.* **38** 441
[20] Hibino Y and Hanafusa H 1983 *Jpn. J. Appl. Phys.* **22** L766
[21] Hanafusa H, Hibino Y and Yamamoto F 1985 *J. Appl. Phys.* **58** 1356
[22] Deschamps T, Vezin H, Gonnet C et al 2013 *Opt. Express* **21** 8382
[23] Chah K, Boizot B, Reynard B et al 2002 *Nucl. Instrum. Methods Phys. Res. Sect. B-Beam Interact. Mater. Atoms* **191** 337